Fano effect and competition between Kondo and antiferromagnetic correlations in double quantum dots

2005 J. Phys.: Condens. Matter 17 1617

(http://iopscience.iop.org/0953-8984/17/10/016)

INSTITUTE OF PHYSICS PUBLISHING JOURNAL OF PHYSICS: CONDENSED MATTER

J. Phys.: Condens. Matter **17** (2005) 1617–1624 doi:10.1088/0953-8984/17/10/016

Fano effect and competition between Kondo and antiferromagnetic correlations in double quantum dots

Zhi-Yong Zhang

Department of Physics, Nanjing University, Nanjing 210093, People's Republic of China

Received 16 December 2004, in final form 28 January 2005
Published 25 February 2005
Online at stacks.iop.org/JPhysCM/17/1617

Abstract

The influence of the Fano effect and the Kondo and antiferromagnetic (AF) correlations on the transport properties through a double quantum dot (DQD) structure is investigated by the finite-U slave-boson mean field method. In the singly-occupied regime, with weak AF correlation, the Fano–Kondo effect greatly reduces the conductance G no matter whether the transmissivity through the direct channel is high or low, whereas the strong parity splitting leads to the blockade of the channel through the DQDs. At the particle–hole symmetric point, when the Kondo and AF correlations are comparable with each other, their competition results in a resonant conductance peak, which is accompanied with a transmission zero due to the Fano effect. This peak-zero structure is a counterpart of the characteristic asymmetric line shape and governs the variational trend of G with the energy levels on dots. The qualitative relations between the positions of those peaks and zeros with the transmissivity through the direct channel are obtained via a fitting method.

1. Introduction

The interplay between quantum interference and the electronic correlation is important in mesoscopic physics. When a discrete energy level is embedded in a continuum energy state, the quantum interference between two configurations—one through the resonant level resulting from the discrete level, and the other directly through the continuum—yields a characteristic asymmetric line shape in the transition rate when the system evolves from an arbitrary initial state. This phenomenon, known as the Fano effect, was proposed first in atomic physics [1] and is observed in many other fields, including condensed matter physics [2–4]. Because of its tunability, quantum dot (QD) systems have attracted a lot of attention. When a dot is connected to leads, the coupling between the localized spin on the dot and conduction electrons leads to the Kondo correlation, which is described by an energy scale T_K, the so-called Kondo temperature. When a dot is in the Kondo regime [5–9], a spin singlet state is formed by the localized spin and conduction electrons. This singlet state yields the Abrikosov–Suhl resonance and plays an important role in the electronic transport. When the Fano effect is introduced in a QD system, the so-called Fano–Kondo effect is found [10–13].

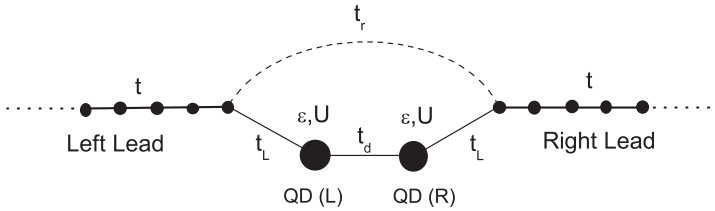

Figure 1. Schematic illustration of the DQD structure.

If double quantum dots (DQDs) [14–17, 21] are coupled with each other by a tunnelling matrix element t_d, the Coulomb interaction U in the dots yields an effective antiferromagnetic (AF) coupling $J_M = \sqrt{(2t_d)^2 + (U/2)^2} - U/2$ (or $\sim 4t_d^2/U$ if $t_d \ll U$). This coupling tends to create a singlet state between the localized spins on the two dots. When the two dots are connected to the left and right leads in a 'lead–dot–dot–lead' series, the competition between the Kondo and AF correlations results in a resonant conductance peak at $J_M \sim T_K$ in the half-filled case [16, 17, 21], whereas in the limit $J_M \ll T_K$ and $t_d \gg U/4$, the conductance G approaches zero. Now, a problem is posed naturally: when the Fano effect is introduced in a DQD system, how does the interplay between the Fano effect and competition between the Kondo and AF correlations affect the transport properties?

In the present paper, we want to answer the following four questions: (i) Does the Fano–Kondo effect still exist if the AF correlation is introduced? (ii) If it does, what are its characteristics in the DQD structure? (iii) Is there a relation exhibiting asymmetric line shape, characterizing the existence of the Fano effect? And (iv) if there is, what are its properties? To this purpose, we assume two QDs (left and right) are tunnelling coupled with each other. A left (right) lead is connected to the left (right) dot, and the two leads are also directly connected by t_r (cf the schematic illustration of the structure in figure 1). To treat the electronic interaction, the finite-U slave boson mean field theory (f-U SBMFT) [18, 19, 21] is adopted. Due to its finite-U character, the AF coupling J_M can be introduced implicitly, unlike in the infinite-U method, where J_M is introduced artificially [15]. In the singly-occupied regime, when $J_M \ll T_K$, the Fano–Kondo effect plays an important role, which greatly reduces G no matter whether t_r is strong or weak, whereas with $t_d \gg U/4$, the strong parity splitting results in the blockade of the path through the DQDs, and the quantum interference effect disappears. At the particle–hole symmetric point, the competition between the Kondo and AF correlations still leads to a resonant peak at $J_M \sim T_K$ as in previous research [16, 17]. But due to the Fano effect, the resonant peak is always accompanied by a transmission zero. This peak-zero structure is a counterpart of the asymmetric line shapes usually found in systems with the Fano effect. By a fitting method, the qualitative relations between t_r and the positions of those peaks and zeros are found. They are $\sim \exp(-bt_r)$ and $\sim 1/t_r$, respectively.

The organization of this paper is as follows. In section 2, the theoretical model and calculation method are illustrated. In section 3, the numerical results and a discussion of them are presented. A brief summary is given in section 4.

2. Model and formulae

In the present paper, we investigate the influence of the Fano effect and the competition between the Kondo and AF correlations on the transport properties through a DQD system at zero temperature. We assume that two dots, labelled as 'L' and 'R', are coupled by a tunnelling matrix element t_d. A left (right) lead is connected to the dot 'L' ('R') via hopping integral $t_L^{(L)}$ ($t_L^{(R)}$) and meanwhile, the two leads are coupled directly to each other via a tunnelling matrix

element t_r. The two QDs are taken as Anderson impurities, each of which has one single-particle energy level and an on-site Coulomb interaction. The two leads are described as two semi-infinite one-dimensional (1D) chains. Then, this mesoscopic system can be described by the following 1D tight-binding Hamiltonian:

$$H = H_L + H_D + H_T, \tag{1}$$

where H_L, H_D and H_T are the Hamiltonians of leads, dots and the coupling between dots and leads. They are

$$H_L = -t\left[\sum_{i=-\infty,\sigma}^{-2} + \sum_{i=1,\sigma}^{\infty}\right](c_{i\sigma}^{\dagger}c_{i+1\sigma} + \text{H.c.}), \tag{2}$$

$$H_D = \sum_{\alpha=L,R}\left(\sum_{\sigma}\epsilon_{\alpha\sigma}c_{\alpha\sigma}^{\dagger}c_{\alpha\sigma} + U_{\alpha}n_{\alpha\uparrow}n_{\alpha\downarrow}\right) - t_d\sum_{\sigma}(c_{L\sigma}^{\dagger}c_{R\sigma} + \text{H.c.}), \tag{3}$$

$$H_T = -\sum_{\sigma}(t_L^{(L)}c_{-1\sigma}^{\dagger}c_{L\sigma} + t_L^{(R)}c_{1\sigma}^{\dagger}c_{R\sigma} + t_r c_{1\sigma}^{\dagger}c_{-1\sigma} + \text{H.c.}). \tag{4}$$

Here the spin index $\sigma = \uparrow$ or $\downarrow$. $\epsilon_{\alpha\sigma}$ and U_α are the energy level and the Coulomb repulsion on the dot 'α', respectively. In the present paper, we consider the left–right symmetric situation and assume spin degeneracy: $\epsilon = \epsilon_{L\sigma} = \epsilon_{R\sigma}$, $U = U_L = U_R$ and $t_L = t_L^{(L)} = t_L^{(R)}$.

If one dot with energy level ϵ and Coulomb repulsion U is connected to the left and right leads with the hopping integral t_L, the Kondo correlation energy, or the Kondo temperature, can be expressed at zero temperature as $T_K = \frac{U\sqrt{J_K}}{2\pi}\exp(-\pi/J_K)$, with $J_K = \frac{-2U\Gamma}{\epsilon(\epsilon+U)}$ [22]. Here, the hybridization strength $\Gamma = \pi\rho(\epsilon_F)t_L^2$, with $\rho(\epsilon_F)$ the density of states at the Fermi energy. The correlation length of a spin singlet at zero temperature $\xi_K = \hbar v_F/T_K$, with v_F the Fermi velocity. In the thermodynamic limit, $\Gamma = 2t_L^2/t$ and $\xi_K = 2t/T_K$ at $\epsilon_F = 0$ [23]. In what follows, we always set $\epsilon_F = 0$. On the other hand, if $t_L^{(L)}$ is set as zero in the Hamiltonian (1), electrons can only tunnel through the structure via the direct channel. At this time, the transmissivity is $|T_r|^2 = 4/(t_r/t + t/t_r)^2$.

The f-U SBMFT of Kotliar and Ruckenstein (KR) [18, 21] is adopted to treat the electronic correlation. It is a powerful nonperturbative tool to study the strongly correlated fermion system, and is not limited to the infinite-U case [24]. In the DQD structure, the AF coupling J_M is introduced implicitly by this method as a function of U and t_d, but not as an artificial parameter in the Hamiltonian [15]. In the framework of this approach, eight auxiliary boson fields e_α, $p_{\alpha\sigma}$ and d_α are introduced, which act as projection operators onto the empty, singly occupied and doubly occupied electronic states at the dot 'α', respectively. To eliminate the unphysical states, six constraints are imposed: $\sum_\sigma p_{\alpha\sigma}^{\dagger}p_{\alpha\sigma} + e_\alpha^{\dagger}e_\alpha + d_\alpha^{\dagger}d_\alpha = 1$ and $c_{\alpha\sigma}^{\dagger}c_{\alpha\sigma} = p_{\alpha\sigma}^{\dagger}p_{\alpha\sigma} + d_\alpha^{\dagger}d_\alpha$. To obtain the correct result in the noninteracting limit, the fermion operator $c_{\alpha\sigma}$ should be replaced by $c_{\alpha\sigma}z_{\alpha\sigma}$, with $z_{\alpha\sigma} = (1 - d_\alpha^{\dagger}d_\alpha - p_{\alpha\sigma}^{\dagger}p_{\alpha\sigma})^{-1/2}(e_\alpha^{\dagger}p_{\alpha\sigma} + p_{\alpha\bar{\sigma}}^{\dagger}d_\alpha)(1 - e_\alpha^{\dagger}e_\alpha - p_{\alpha\bar{\sigma}}^{\dagger}p_{\alpha\bar{\sigma}})^{-1/2}$. Therefore the Hamiltonian (1) can be replaced by the following effective Hamiltonian:

$$H_{\text{eff}} = H_L + \tilde{H}_D + \tilde{H}_T + \sum_{\alpha=L,R}\left\{\lambda_\alpha^{(1)}\left(\sum_\sigma p_{\alpha\sigma}^{\dagger}p_{\alpha\sigma} + e_\alpha^{\dagger}e_\alpha + d_\alpha^{\dagger}d_\alpha - 1\right)\right.$$
$$\left. + \sum_\sigma \lambda_{\alpha\sigma}^{(2)}(c_{\alpha\sigma}^{\dagger}c_{\alpha\sigma} - p_{\alpha\sigma}^{\dagger}p_{\alpha\sigma} - d_\alpha^{\dagger}d_\alpha)\right\}, \tag{5}$$

where the six constraints are incorporated by the six Lagrange multipliers $\lambda_\alpha^{(1)}$ and $\lambda_{\alpha\sigma}^{(2)}$. The original H_D and H_T are changed to

$$\tilde{H}_D = \sum_{\alpha=L,R}\left(\sum_\sigma \epsilon_{\alpha\sigma}c_{\alpha\sigma}^{\dagger}c_{\alpha\sigma} + U_\alpha d_\alpha^{\dagger}d_\alpha\right) - t_d\sum_\sigma(z_{L\sigma}^{\dagger}c_{L\sigma}^{\dagger}c_{R\sigma}z_{R\sigma} + \text{H.c.}) \tag{6}$$

and

$$\tilde{H}_{\rm T} = -\sum_{\sigma}(t_{\rm L}c^{\dagger}_{-1\sigma}c_{{\rm L}\sigma}z_{{\rm L}\sigma} + t_{\rm L}c^{\dagger}_{1\sigma}c_{{\rm R}\sigma}z_{{\rm R}\sigma} + t_{\rm r}c^{\dagger}_{1\sigma}c_{-1\sigma} + {\rm H.c.}), \tag{7}$$

whereas $H_{\rm L}$ remains unchanged.

To solve the effective Hamiltonian (5), we can integrate out the fermionic variables from the corresponding effective action, write down the saddle-point free-energy functional, and then determine the expectation values of the boson fields by minimization of the saddle-point free-energy functional at zero temperature as KR did in their original paper [18]. But, this approach is equivalent to a mean-field approximation in which the slave boson fields are first replaced by their expectation values, then the values of e_α, $p_{\alpha\sigma}$, d_α, $\lambda^{(1)}_\alpha$ and $\lambda^{(2)}_{\alpha\sigma}$ are obtained by minimization of the ground state energy E_0 of the essentially noninteracting effective Hamiltonian (5) with respect to these parameters [19]. This leads to a set of self-consistent equations [19, 21]. Because of the left–right symmetry and the spin degeneracy, only five variational parameters need to be determined. They are e, p, d, $\lambda^{(1)}$ and $\lambda^{(2)}$. To construct the five self-consistent equations, we need knowledge of the ground state $|0\rangle$. This is obtained from the calculation of a cluster, at the centre of which is located the DQD structure. The single-particle eigenstates can be calculated by direct numerical diagonalization, and the ground state $|0\rangle$ is constructed by adding electrons to the lowest unoccupied levels one by one up to the Fermi level. If the cluster size is much larger than $\xi_{\rm K}$, the results obtained from the cluster calculation can be looked upon as those of the original system [25, 26].

As soon as the five variational parameters are obtained, the conductance G through the structure at zero temperature can be obtained from the Landauer–Büttiker's (LB) formula $G = |T(\epsilon_{\rm F})|^2$, because the effective Hamiltonian (5) is essentially noninteracting [27]. Here $T(\epsilon_{\rm F})$ is the transmission coefficient of an incident electron with the Fermi energy. In writing the above equation, the spin index and the unit $2e^2/h$ are omitted. The applicability of the LB formula would not be destroyed by the inclusion of the direct hopping between the left and right leads or the external applied ac voltage [20]. For continuum models, some authors adopted the LB formula combined with the slave-boson mean-field method to calculate G via the Green function technique [12, 21]. But for a tight-binding Hamiltonian, the transmission coefficient T can be calculated more straightforwardly via the transfer matrix (TM) method [28, 29]. The transfer matrices corresponding to the effective noninteracting Hamiltonian (5) hold the same forms as those corresponding to the original Hamiltonian (1) when the Coulomb interaction U is set as 0 in equation (1). In the mean-field approximation, the electron–electron interaction is represented in the transfer matrices by the replacement of the undressed parameters by the renormalized ones: $\tilde{\epsilon} = \epsilon + \lambda^{(2)}$, $\tilde{t}_{\rm d} = t_{\rm d}z^2$ and $\tilde{t}_{\rm L} = t_{\rm L}z$. This situation is similar to that in the conductance calculation via the Green function technique [12, 21],

3. Results and discussion

The variations of G with ϵ for different $t_{\rm d}$ are plotted in figures 2(a)–(c). We first give our attention to the results with $t_{\rm r} = 0$, which are given in figure 2(a), and compare them with the exact numeric results. For any $t_{\rm d}$, the G–ϵ curves are symmetrical with $\epsilon = -U/2$. For $t_{\rm d} = 0.01$ and 0.1 (here, we set $t = 1$), a plateau is found in the singly-occupied regime $-U < \epsilon < 0$, and its height value with $t_{\rm d} = 0.1$ is close to unity, whereas that with $t_{\rm d} = 0.01$ is close to zero. For $t_{\rm d} = 0.2$, 0.4 and 0.8, the plateau splits into two resonant peaks, and with $t_{\rm d}$ increased, the splitting is strengthened and the G value at $\epsilon = -U/2$ decreases. For any $t_{\rm d}$, in the empty and doubly-occupied regimes, G always approaches zero. In our calculations, $U = 1.4$ and $t_{\rm L} = 0.35$, so $T_{\rm K}$ and $\xi_{\rm K}$ are 0.0280 and 71.5, respectively, at the particle–hole

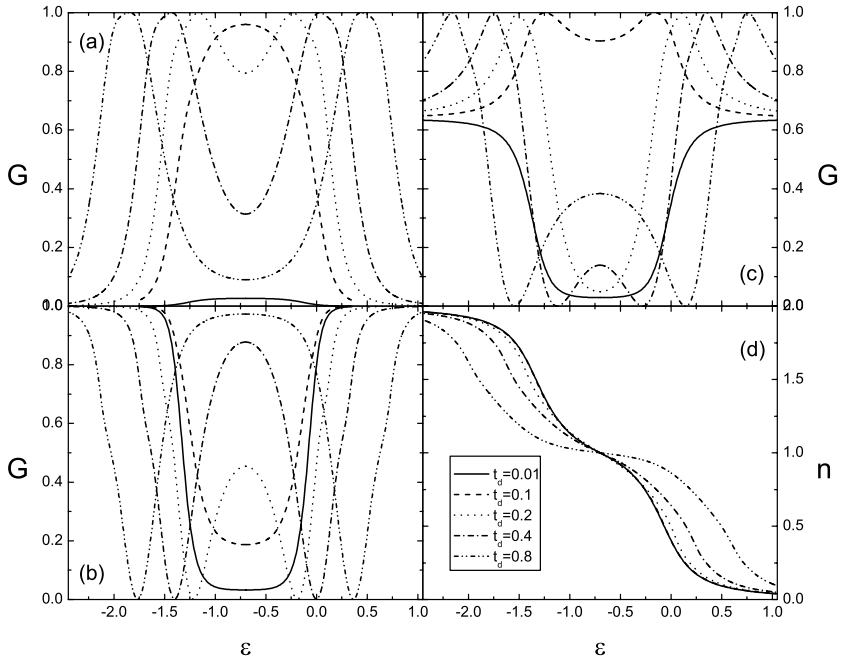

Figure 2. G–ϵ curves with different $t_{\rm d}$ for $t_{\rm r} = 0$ (a), 1 (b) and 0.5 (c). (d) n–ϵ curves with different $t_{\rm d}$ for $t_{\rm r} = 0$. In this figure, the curves with the same texture have the same $t_{\rm d}$. The other parameters are $U = 1.4$ and $t_{\rm L} = 0.35$.

Table 1. Table of $J_{\rm M} = \sqrt{(2t_{\rm d})^2 + (U/2)^2} - U/2$ with $U = 1.4$. When $t_{\rm L} = 0.35$, $T_{\rm K} = 0.0280$, which is almost identical to the $J_{\rm M}$ at $t_{\rm d} = 0.1$.

$t_{\rm d}$	0.01	0.1	0.12	0.2	0.4	0.8
$J_{\rm M}$	2.86×10^{-4}	0.0280	0.0400	0.106	0.363	1.05

symmetric point $\epsilon = -U/2$. Here the lattice constant $a = 1$. To guarantee good convergence, the cluster size is set as 800 with $t_{\rm d} < 0.1$, 400 with $0.1 \leqslant t_{\rm d} < 0.2$ and 200 with $0.2 \leqslant t_{\rm d}$ in the determination of the variational parameters.

In figure 2(d), the variation of the electronic occupation number n on each dot with ϵ is plotted with $t_{\rm r} = 0$. For $t_{\rm d} = 0.01$, $J_{\rm M} \ll T_{\rm K}$, the Kondo effect prevails, and in the singly-occupied regime, n varies slowly. The values of $J_{\rm M}$ for a series of $t_{\rm d}$ are given in table 1. For $t_{\rm d} = 0.1$, $J_{\rm M} \simeq T_{\rm K}$, and the structure is close to the resonant point. For $t_{\rm d} = 0.2$, $J_{\rm M} > T_{\rm K}$, and the AF correlation dominates. But in both of these two cases, the n–ϵ curves are close to that for $t_{\rm d} = 0.01$. As a comparison, when $t_{\rm d} = 0.4$ and 0.8, the n–ϵ curves become flat in the singly-occupied regime. This phenomenon is more remarkable for $t_{\rm d} = 0.8$. This is because when $t_{\rm d} > U/4$, the parity splitting leads to the double occupancy on the bonding orbital of the two dots, which tends to block the electronic transport. In figure 3, the G–$t_{\rm d}$ curve with $t_{\rm r} = 0$ is given by the solid curve at $\epsilon = -U/2$. With $t_{\rm d} \to 0$ and ∞, G always approaches zero. A resonant peak emerges at $t_{\rm d}^{\rm R} = 0.12$. The corresponding $J_{\rm M} = 0.04 \sim T_{\rm K}$. All of these are consistent with the exact numeric results [16, 17], and although it is a mean-field method, the f-U SBMFT grasps the basic physics of the DQD structure. Now, we turn our attention to the situation with $t_{\rm r} \neq 0$.

In figures 2(b) and (c), we plot the G–ϵ curves for different $t_{\rm d}$ with $t_{\rm r} = 1$ and 0.5, respectively. But here, we do not give the corresponding n–ϵ curves, because the introduction

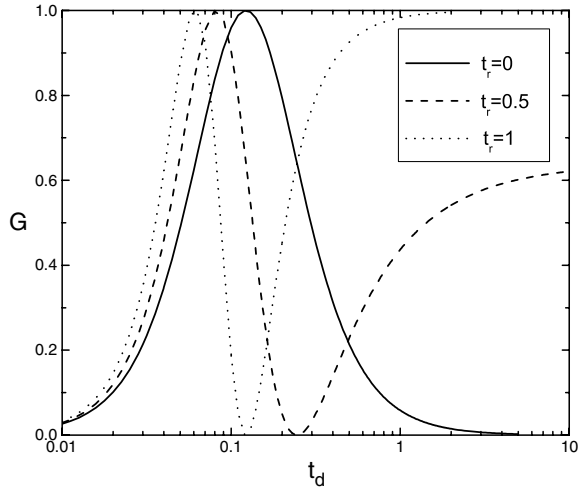

Figure 3. G–t_d curves with $\epsilon = -U/2$ for $t_\mathrm{r} = 0$ (solid), 0.5 (dashed) and 1 (dotted).

of t_r only has small influence on the n–ϵ curves. This demonstrates that the direct tunnelling cannot eliminate the Kondo or AF correlations in the system and their competition still plays an important role. But the direct tunnelling introduces the quantum interference between different channels. As in the single QD situation [10, 11], G always approaches $|T_\mathrm{r}|^2$ when $|\epsilon| > U$. (Here, $|T_\mathrm{r}|^2 = 0.64$ for $t_\mathrm{r} = 0.5$.) For $t_\mathrm{r} = 0.5$, in the G–ϵ curves with $t_\mathrm{d} = 0.4$ and 0.8 there are two resonant peaks and two transmission zeros, but in the curves with $t_\mathrm{d} = 0.1$ and 0.2 only two resonant peaks appear, and with $t_\mathrm{d} = 0.01$ neither resonant peak nor transmission zero emerges. The peak and/or zero structures can only appear with certain t_d, and if they appear, they appear in a pair and are located at the symmetric positions with respect to the point $\epsilon = -U/2$. This leads to symmetric G–ϵ curves. The same character is also found for $t_\mathrm{r} = 1$, but here, the resonant peaks are merged into the tails with unit conductance. This is entirely different from the single QD system, where one resonant peak and one transmission zero always appear simultaneously and they are located at the opposite sides of the particle–hole symmetric point, which leads to asymmetric G–ϵ curves.

To find the underlying rule governing the appearance of peaks and zeros, we also present the corresponding G–t_d curves with $\epsilon = -U/2$ for $t_\mathrm{r} = 0.5$ and 1 in figure 3. They are plotted with dashed and dotted curves, respectively. For any t_r, G approaches zero if t_d is close to zero. This is a clear demonstration of the Fano–Kondo effect: if $t_\mathrm{d} = 0$, the two dots are decoupled from each other and can be looked upon as side-coupled to a 1D chain, and G through this structure is zero in the Kondo regime no matter whether the direct tunnelling is strong or weak [12]. When t_d is introduced, the Kondo correlation still dominates and that kind of Fano–Kondo effect plays a major role if $J_\mathrm{M} \ll T_\mathrm{K}$. This accounts for the appearance of the low plateau in the singly-occupied regime with $t_\mathrm{d} = 0.01$ in figures 2(b) and (c). With $J_\mathrm{M} \sim T_\mathrm{K}$, the competition between the Kondo and AF correlations leads to a resonant peak in the G–t_d curves. But the most striking change on a G–t_d curve caused by the introduction of t_r is the appearance of a transmission zero accompanied with the resonant peak. This is a demonstration of the interplay between the Fano effect and the competition of the Kondo and AF correlations. The peak-zero structure is very similar to the asymmetric line shapes usually found in other systems with Fano effect. If the positions of peaks and zeros are set as t_d^R and t_d^D, respectively, in the G–ϵ curves (cf figure 2), only when $t_\mathrm{d} > t_\mathrm{d}^{\mathrm{R(D)}}$ do two resonant

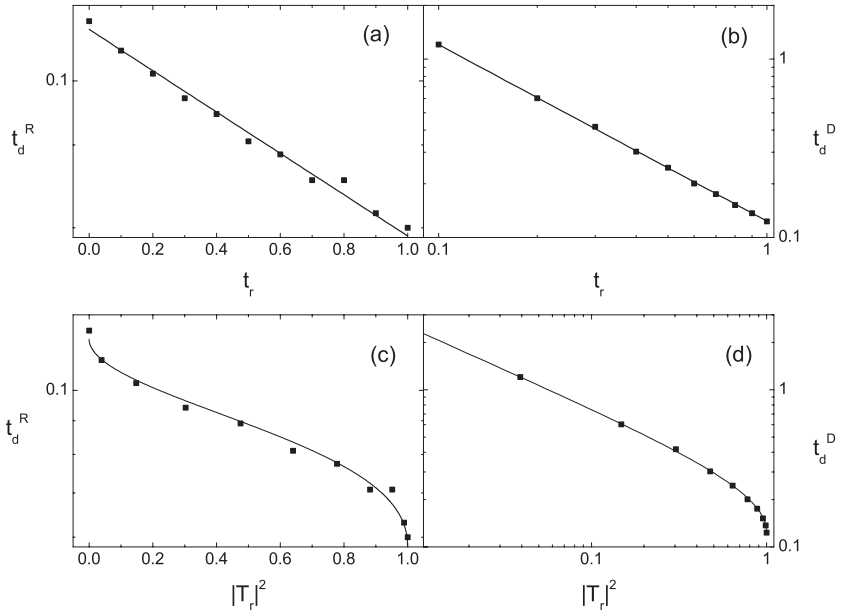

Figure 4. Relations of t_d^R and t_d^D with t_r ((a) and (b)) and with $|T_r|^2$ ((c) and (d)). The data obtained from the f-U SBMFT are represented as filled rectangles and the solid lines correspond to the fitting functions.

peaks (transmission zeros) appear in symmetrical positions with respect to $\epsilon = -U/2$. In the G–t_d curves, with t_d further increased, G approaches $|T_r|^2$, the transmissivity through the direct channel. In this regime, the strong parity splitting leads to the double occupancy on the bonding orbital. This results in the blockade of the channel through the DQDs, and the quantum interference disappears.

Variation of t_r only slightly changes t_d^R: it is 0.12 for $t_r = 0$ whereas it is 0.061 for $t_r = 1$. But the change of t_d^D is great: for $t_r = 0$, it can be set as infinity, which is contrasted with the corresponding value 0.12 for $t_r = 1$. For any t_r, t_d^D is always larger than t_d^R. This explains why the two resonant peaks always appear on the outside of the two transmission zeros in the G–ϵ curves. Figures 4(a) and (b) give the variation relations of t_d^R and t_d^D with t_r, where our f-U SBMFT data are represented as filled rectangles, and the solid lines are the corresponding fitting functions. They are $t_d^R = a\exp(-bt_r)$ and $t_d^D = c/t_r$, respectively. The three parameters can be determined as $a = 0.119$, $b = 0.72$ and $c = 0.123$. Here a and c are very close to each other. Figures 4(c) and (d) present the same results as (a) and (b) but with t_r replaced by $|T_r|^2$ since $|T_r|^2$ is the experimentally measurable value. In the limit of $|T_r|^2$ approaching zero, t_d^R and t_d^D exhibit the following behaviours: $t_d^D \sim 1/\sqrt{|T_r|^2}$, and $\ln(t_d^R) \sim -\sqrt{|T_r|^2}$. However, in the limit of $|T_r|^2$ approaching unity, $t_d^D \sim \sqrt{|T_r|^2}$ and $\ln(t_d^R) \sim -1/\sqrt{|T_r|^2}$. Of course, these results are obtained from the f-U SBMFT. The accurate values of those fitting parameters can only be determined by more powerful methods, but we hope that the qualitative relations found by our calculation can be verified by experiments.

In the above theoretical calculation, left–right symmetry is assumed: $\epsilon_L = \epsilon_R$. When an energy difference $\delta = \epsilon_L - \epsilon_R$ is introduced, the left–right asymmetry appears besides the asymmetry caused by the parity splitting. As in the case of the parity splitting, when $\delta < U/4$, the influence of the left–right asymmetry is negligible. Only when $\delta > U/4$ do remarkable differences appear between the structures with and without left–right symmetry.

4. Summary

In summary, we have investigated the influence of the Fano effect and the Kondo and AF correlations on the transport properties through a DQD structure by the f-U SBMFT. When $J_M \ll T_K$, the Fano–Kondo effect plays an important role, which greatly reduces G in the singly-occupied regime no matter whether t_r is strong or weak. In contrast, when $t_d \gg U/4$, the channel through the DQDs is blocked because of parity splitting, and G is just $|T_r|^2$. From the variation of G at the particle–hole symmetric point with t_d, it can be found that the competition between the Kondo and AF correlations leads to a resonant peak at $J_M \sim T_K$ as in previous research [16, 17]. But due to the Fano effect, the resonant peak is always accompanied by a transmission zero. This peak-zero structure is similar to the asymmetric line shapes usually found in systems with the Fano effect. This structure also governs the basic shape of the G–ϵ curves. By a fitting method, the qualitative relations of t_d^R and t_d^D with t_r are found. They are $t_d^R \sim \exp(-bt_r)$ and $t_d^D \sim 1/t_r$, respectively. These two relations are also expressed with t_r replaced by $|T_r|^2$.

Acknowledgments

The author acknowledges the support by National Foundation of Natural Science in China Grant No 10204012, and by the special funds for Major State Basic Research Project No G001CB3095 of China.

References

[1] Fano U 1961 *Phys. Rev.* **124** 1866
[2] Göres J *et al* 2000 *Phys. Rev.* B **62** 2188
[3] Zacharia I G *et al* 2001 *Phys. Rev.* B **64** 155311
[4] Kobayashi K, Aikawa H, Katsumoto S and Iye Y 2002 *Phys. Rev. Lett.* **88** 256806
[5] Goldhaber-Gordon D, Shtrikman H, Mahalu D, Abusch-Magder D, Meirev U and Kaster M A 1998 *Nature* **391** 156
[6] Cronewett S M, Oosterkamp T H and Kouwenhoven L P 1998 *Science* **281** 540
[7] Simmel F, Blick R H, Kotthaus U P, Wegsheider W and Blichler M 1999 *Phys. Rev. Lett.* **83** 804
[8] van der Wiel W G, De Franceschi S, Fujisawa T, Elzerman J M, Tarucha S and Kouwenhoven L P 2000 *Science* **289** 2105
[9] Ji Y, Heiblum M, Sprinzak D, Mahalu D and Shtrikman H 2000 *Science* **290** 779
[10] Hofstetter W, König J and Shoeller H 2001 *Phys. Rev. Lett.* **87** 156803
[11] Bulka B R and Stefanski P 2001 *Phys. Rev. Lett.* **86** 5128
[12] Kang K, Cho S Y, Kim J J and Shin S C 2001 *Phys. Rev.* B **63** 113304
[13] Franco R, Figueira M S and Anda E V 2003 *Phys. Rev.* B **67** 155301
[14] Aono T, Eto M and Kawamura K 1998 *J. Phys. Soc. Japan* **67** 1860
[15] Georges A and Meir Y 1999 *Phys. Rev. Lett.* **82** 3508
[16] Büsser C A, Anda E V, Lima A L, Davidovich M A and Chiappe G 2000 *Phys. Rev.* B **62** 9907
[17] Izumida W and Sakai O 2000 *Phys. Rev.* B **62** 10260
[18] Kotliar G and Ruckenstein A E 1986 *Phys. Rev. Lett.* **57** 1362
[19] Dorin V and Schlottmann P 1993 *Phys. Rev.* B **47** 5095
[20] Ma Z, Zhu Y, Li X-Q, Lin T-H and Su Z-B 2004 *Phys. Rev.* B **69** 045302
[21] Dong B and Lei X L 2002 *Phys. Rev.* B **65** 241304
[22] Hewson A C 1993 *The Kondo Problem to Heavy Fermions* (Cambridge: Cambridge University Press)
[23] Kang K and Shin S-C 2000 *Phys. Rev. Lett.* **85** 5619
[24] Coleman P 1984 *Phys. Rev.* B **29** 3035
[25] Affleck I and Simon P 2001 *Phys. Rev. Lett.* **86** 2854
[26] Hu H, Zhang G-M and Yu L 2001 *Phys. Rev. Lett.* **86** 5558
[27] Meir Y and Wingreen N S 1992 *Phys. Rev. Lett.* **68** 2512
[28] Simon P and Affleck I 2003 *Phys. Rev.* B **68** 115304
[29] Xiong S J and Evangelou S N 1995 *Phys. Rev.* B **52** 13079